1

Multiplexed live-cell visualization of endogenous proteins with nanometer precision by fluorobodies

Alina Klein[1], Susanne Hank[1], Anika Raulf[2], Felicitas Tissen[1], Mike Heilemann[2], Ralph Wieneke[1]*, and Robert Tampé[1,3]*

[1] Institute of Biochemistry, Biocenter, Goethe University Frankfurt, Max-von-Laue Str. 9, 60438 Frankfurt/Main, Germany; [2] Institute of Physical and Theoretical Chemistry, Goethe University Frankfurt, Max-von-Laue Str. 7, 60438 Frankfurt/Main, Germany; [3] Cluster of Excellence - Macromolecular Complexes, Goethe University Frankfurt, Max-von-Laue Str. 9, 60438 Frankfurt/Main, Germany

*Correspondence should be addressed to R.W. (wieneke@em.uni-frankfurt.de) or R.T. (tampe@em.uni-frankfurt.de)

Abstract: 129 words | **Main text**: 2,411 words | **Figures:** 3 | **Supplemental Figures:** 15

Key words: endogenous protein labeling, *in vivo* labeling, live-cell imaging, nanobody, super-resolution microscopy

1 Abstract

2 The visualization of endogenous proteins in living cells is a major challenge. A fundamental

3 requirement for spatiotemporally precise imaging is a minimal disturbance of protein function at

4 high signal-to-background ratio. Current approaches for visualization of native proteins in living

5 cells are limited by dark emitting, bulky fluorescent proteins and uncontrollable expression levels.

6 Here, we demonstrate the labeling of endogenous proteins using nanobodies with site-specifically

7 engineered bright organic fluorophores, named fluorobodies. Their fast and fine-tuned intracellular

8 transfer by microfluidic cell squeezing allowed for low background, low toxicity, and high-

9 throughput. Multiplexed imaging of distinct cellular structures was facilitated by specific protein

10 targeting, culminating in live-cell super-resolution imaging of protein networks. The high-

11 throughput delivery of engineered nanobodies will open new avenues in visualizing native cellular

12 structures with unprecedented accuracy in cell-based screens.

Introduction

The localization of endogenous proteins in native settings is fundamental for quantitative spatiotemporal understanding of cellular homeostasis and dysfunction. Here, live-cell imaging is highly desired to visualize timely-balanced protein networks, avoiding contingent artifacts by fixation or permeabilization procedures.[1] In this regard, genetic fusion of fluorescent proteins (FPs) enabled the visualization of proteins of interest (POIs).[2] However, the fusion to FPs or other bulky enzyme-based tags (*e.g.* SNAP$_f$ tag)[3] can provoke protein misassembly, mistargeting, and overexpression artifacts.[4] Alternatively, antibodies and recombinant binders are prominent tools to trace proteins.[5-8] Yet, targeting with conventional antibodies is limited to fixed cells since their disulfide bonds are reduced in the cytosol. To overcome this downside, antibody fragments have been developed for protein targeting.[9,10] For in-cell labeling of endogenous proteins, the binder must fulfill several demands: high affinity and specificity to its target, long-term stability in the reducing milieu of the cytosol, and small size avoiding interference with the POI's function. In this light, the variable domains of heavy-chain only antibodies (V$_H$Hs) of camelids, named nanobodies, are prime candidates.[11,12] They bind with nanomolar or even picomolar affinities to their targets, are very small in size (~ 13 kDa), exhibit great solubility, and can be functionally produced in the reducing cytosolic milieu of mammalian cells. Nanobodies fused to fluorescent proteins (chromobodies) have been used to trace various POIs.[12-18] Recently, a chromobody has been developed for actin labeling in the cytosol and nucleus of mammalian cells,[19] surpassing common techniques such as LifeAct by minimizing interference with actin dynamics.[20] Nonetheless, visualization of intracellular proteins is still impeded because fused FPs triple the size of the nanobody and FPs entail suboptimal photophysical properties for super-resolution microscopy. An additional drawback of chromobodies is that their expression level cannot be precisely controlled, evoking high background and deteriorated signal-to-background staining, which in turn makes the observation of low abundant proteins and in particular super-resolution microscopy very difficult or impossible. As recently demonstrated, nanobodies directed against FPs were

3

1   equipped with quantum dots or organic dyes to trace kinesin by single-particle tracking.[21,22]

2   However, both studies were limited by the expression of a genetically modified POI.

3   So far, methods visualizing endogenous proteins in live unmodified cells have not been

4   accomplished. To overcome this limitation, we advanced nanobodies with bright, high-

5   performance fluorescent probes, named fluorobodies. Combined with high-throughput cellular

6   delivery by a vector-free microfluidic device,[23,24] endogenous proteins were visualized by multi-

7   color imaging at excellent signal-to-background ratios. Ultimately, the endogenous nuclear lamina

8   was resolved at nanometer precision by live-cell super-resolution microscopy.

9

Results

Specific protein labeling *via* fluorobodies

12   As a first showcase, we modified the established α-GFP nanobody[25,26] by strategic positioning of

13   small organic fluorescent probes. We engineered nanobodies with a single free cysteine either at

14   the N or C terminus, or position 9, respectively. After expression and affinity purification, the

15   nanobodies were labeled via maleimide coupling with high-quantum yield fluorophores of, *e.g.*

16   sulfo-Cyanine 3 (sCy3), sCy5, or ATTO655 (**Figure 1a**). To suppress transient exposure of inner

17   scaffold cysteines by thermal breathing, covalent dye attachment was performed at 4 °C.[27]

18   Specific conjugation of the fluorophore was confirmed by SDS-PAGE in-gel fluorescence and

19   fluorescence-detection size-exclusion chromatography, with molar labeling ratios of ~ 0.9 for

20   α-GFP^{sCy3} and ~ 0.8 for α-GFP^{sCy5} (**Figure 1b** and **Figure 1 – Figure Supplement 1**).

21   As an initial screen, we evaluated specific binding of the α-GFP fluorobodies (Fbs) in fixed cells

22   prior to live-cell applications. Different intracellular assemblies were selected as targets, *e.g.* the

23   transporter associated with antigen processing TAP (TAP1-mVenus) in the ER membrane,

24   histone 2B (H2B-EGFP) in the nucleus, and lamin A (mEGFP-Lamin A) as a component of the

1   nuclear envelope. The respective POIs were expressed in human HeLa Kyoto cells, labeled with

2   the α-GFP Fbs (50-200 nM) and analyzed by confocal laser scanning microscopy (CLSM). The

3   Fbs retained high target specificity with negligible background staining (**Figure 1c,d** and **Figure 1**

4   **– Figure Supplement 2**). More important, an excellent co-localization was observed as depicted

5   by Pearson's coefficients ranging from 0.948 to 0.986, independently of the attached synthetic

6   dyes (sCy3 and sCy5; **Figure 1c,d** and **Figure 1 – Figure Supplement 2**). The Fb intensity

7   distribution highly correlated with the POI expression level, reflecting specific and stoichiometric

8   binding (**Figure 1e** and **Figure 1 – Figure Supplement 2** and **3**).

9   To avoid limitations typically entailed by overexpression of fusion proteins, we traced the

10   endogenous nuclear envelope by an engineered α-Lamin Fb. As basic constituents of the nuclei,

11   lamins are assembled in a filamentous meshwork, providing structural stability. Importantly, only

12   after nanobody production in an *E. coli* strain, engineered to promote disulfide bond formation in

13   the cytosol, and application of an optimized coupling procedure, specific labeling of the

14   endogenous nuclear lamina was facilitated with α-Lamin Fbs equipped with sCy5 or ATTO655 at

15   labeling ratios of 0.8 to 1.0, respectively. Noteworthy, different procedures led to successful dye

16   conjugation, but were accompanied with loss in specificity (**Figure 1 – Figure Supplement 4**).

17   Similar results were obtained if lysine residues on the nanobody surface were stochastically

18   modified via *N*-hydroxysuccinimide (NHS) Alexa647 (**Figure 1 – Figure Supplement 4a**).

19   Contrary, the α-GFP Fb always retained high target specificity in fixed cells, independent of all

20   described routes for production and labeling (**Figure 1 – Figure Supplement 5**). Since the highest

21   signal-to-background ratio was achieved after dye-conjugation to the N-terminal cysteine of the

22   α-Lamin Fb (**Figure 1f,g**; **Supplementary Video 1** and **Figure 1 – Figure Supplement Fig. 4**),

23   labeling at this position was employed for all further experiments.

1 **Live-cell protein labeling at nanomolar fluorobody concentrations**

2 Once the specificity in fixed cells was proven, we aimed at live-cell protein labeling. For the fast

3 and efficient Fb transfer, we made use of high-throughput, microfluidic cell squeezing. Here,

4 transient pore formation of the plasma membrane is induced by forcing cells through micrometer

5 constrictions of microfluidic devices (**Figure 2 – Supplement Figure 1**). This approach has shown

6 to bypass endosomal uptake and offered precise control of the transduced cargo concentration

7 combined with high-throughput delivery (1,000,000 cells/s) and minimal cytotoxicity (< 10%).[23,24]

8 Initially, α-GFP Fbs were delivered into HeLa Kyoto cells expressing the three selected FP-tagged

9 proteins and the intracellular Fb distribution was analyzed 1 to 3 h after cell transfer. In all cases,

10 the fluorescence of the α-GFP Fb showed a high degree of co-localization with FP-tagged H2B,

11 TAP1, or lamin A, reflected by Pearson's coefficients ranging from 0.864 to 0.911 (**Figure 2a** and

12 **Figure 2 – Supplement Figure 2a**). Exemplary, an excellent correlation between the fluorescence

13 intensity profiles of TAP1-mVenus and the α-GFP[sCy3] Fb was observed (**Figure 2b**,**c**; Pearson's

14 coefficient of 0.926). Notably, all transduced cells displayed a very low background staining and

15 the intensity of the Fb reflected the variability in the POI expression level. We observed an

16 increased Fb binding in cells with high levels of FP-tagged POIs, whereas cells expressing low

17 amounts of the POIs displayed weaker fluorescence intensities (**Figure 2 – Supplement**

18 **Figure 3**). One explanation for this correlation is found in the release of unbound binders during

19 membrane resealing as well as in the nanomolar concentration of Fbs in the squeezing buffer,

20 both synergistically contributing to a high signal-to-background staining (**Figure 2d**).[22] Indeed,

21 untransfected cells indicated a very low level of uniformly intracellular distributed Fbs (**Figure 2 –**

22 **Supplement Figure 4**). This is in line with the localization of the α-GFP-mCherry chromobody or

23 mCherry expressed in HeLa Kyoto cells (**Figure 2 – Supplement Figure 5a,b**). In contrast,

24 expression of α-GFP-mCherry chromobodies together with FP-tagged POIs often resulted in

25 overabundance of the binder due to mismatched expression levels (**Figure 2 – Supplement**

26 **Figure 5c-e**). Here, a high signal-to-background labeling is impaired in cells with high expression

1   levels of chromobodies, while very low levels entail high sensitivity to photobleaching. These

2   drawbacks were successfully abolished by microfluidic Fb transfer. To test the long-term stability

3   and persistence of Fb labeling, cells were imaged 20 h after transduction. Remarkably, the POIs

4   were still decorated by α-GFP Fbs, highlighting their long-term specificity and in-cell robustness

5   (**Figure 2 – Supplement Figure 2**). Over time, however, cytosolic punctae and a higher

6   background signal were detected, indicating incipient Fb degradation. Collectively, the adaptive,

7   fine-tuned intracellular delivery of Fbs by cell squeezing promoted low-background labeling of

8   genetically tagged proteins.

9

10   **High signal-to-background tracing of endogenous proteins in live mammalian cells**

11   We next focused on live-cell labeling of endogenous protein networks. With regard to their

12   extenuated abundance, the utilization of high-performance fluorescent or fluorogenic probes is

13   essential to enhance sensitivity. We selected two intermediate filaments as targets. Specifically,

14   we used the engineered α-Lamin Fb to visualize the native lamin meshwork of the nuclear

15   envelope and α-Vimentin^{ATTO488} for tracing vimentin as a cytoskeletal component, crucial for

16   organelle positioning. Target specificity of both Fbs was verified beforehand in fixed cells

17   (**Figure 1f,g** and **Figure 3 – Supplement Figure 1**). In live HeLa Kyoto cells expressing

18   α-Lamin-EGFP chromobody, decoration of the nuclear lamina was accompanied with high

19   background staining and cytosolic punctae, presumably due to saturation of the targeting

20   machinery (**Figure 3 – Supplement Figure 2**). Contrarily, specific decoration of endogenous

21   lamin with a concomitant negligible background was visualized 3 h after cell squeezing utilizing

22   the α-Lamin^{ATTO655} Fb (**Figure 3a**). To the best of our knowledge this constitutes the first labeling

23   of an endogenous protein inside living cells by Fbs. Notably, even 20 h after cell squeezing,

24   labeling of the nuclear lamina was still persistent. Nevertheless, higher background, mainly as

25   cytosolic punctae, was observed (**Figure 3 – Supplement Figure 3**), in line with results obtained

1   for the α-GFP Fb (**Figure 2 – Supplement Figure 2b**). Of note, specific targeting was unaffected

2   by the utilized fluorophore (ATTO655 or sCy5; **Figure 3a** and **Figure 3 – Supplement Figure 3**).

3   To further broaden the range of applications, α-Vimentin^{ATTO488} was delivered into cells. The well-

4   defined filamentous structure of endogenous vimentin was visualized with a high signal-to-

5   background ratio 3 h as well 20 h after cell squeezing (**Figure 3b,c** and **Figure 3 – Supplement**

6   **Figure 4**).

7

8   **Multiplex and super-resolution analysis of native cellular protein networks**

9   Encouraged by these results, we performed multi-color live-cell labeling by combining both

10   binders. 3D mapping of cell topology via multiplexed imaging revealed simultaneous and specific

11   decoration of the nuclear lamina (**Figure 3d**, red) and vimentin filaments (**Figure 3d**, green) at

12   endogenous level, hardly realized by multiple knock-ins utilizing the CRISPR/Cas9 technology.

13   The spatial distinct distribution allowed discriminating between both structures by live-cell

14   immunofluorescence imaging. In combination with their precisely adjusted delivery by cell

15   squeezing, the small Fbs, site-specifically labeled with minimal and bright fluorescent dyes

16   (≤ 1 nm) provides an excellent showcase for live-cell super-resolution microscopy. Consequently,

17   α-Lamin^{ATTO655} Fb transduced cells were subjected to *direct* stochastic optical reconstruction

18   microscopy (*d*STORM).[28] We obtained images of the endogenous nuclear lamina in living cells

19   with an average resolution of ~ 55 nm (localization precision of 23.4 ± 8.3 nm; **Figure 3e**) and

20   significantly increased contrast compared to wide-field imaging (**Figure 3f**). Strikingly, *d*STORM

21   analysis of α-Lamin^{ATTO655} Fb in fixed cells yielded virtually identical average localization precision,

22   but an increased signal-to-background-ratio was obtained in living cells, devoid of fixation artifacts

23   (**Figure 3 – Supplement Figure 5**).

Discussion

In general, the much lower level of endogenous proteins makes their specific and low-background tracing very challenging. To circumvent this constrain, we established a method for live-cell visualization of endogenous proteins at nanometer resolution and with minimal disturbance and high reproducibility (n ≥ 3 for every POI). This robust and generic technique is versatile in the choice of the nanobody and bright organic fluorophore and allows for low-background tracing of high as well as low abundant native protein networks in living cells. In case of our selected target structures, Fb decoration was persistent for several hours after Fb transfer. However, increased background after 20 h suggests that long-term protein tracing can be affected. This obstacle is experimentally manageable, depending on the turnover rate of the POI as well as the rate of cell division. Alternative approaches to tag endogenous proteins such as the generation of stable cell lines utilizing *e.g.* CRISPR/Cas9 for low chromobody levels are highly promising, yet very labor-intensive and hardly realizable for multiple knock-ins.

Collectively, our devised strategy strikes a new path for the live-cell visualization of endogenous targets by high quantum yield fluorobodies to study their precise intracellular localization and trafficking. The simplicity and robustness of the methodology can be extended to deliver multiple probes simultaneously for multiplexed imaging and has tremendous potential for other types of microscopy (*e.g.* electron microscopy). Even the Fb targeting of endogenous proteins in embryonic stem cells or patient-derived primary immune cells is technically feasible via cell squeezing. Moreover, our method provides access of exogenously derived high-affinity binding scaffolds (*e.g.* fibronectin-based binding proteins or designed ankyrin repeat proteins) for 3D and multi-color super-resolution imaging in native cells and opens avenues to label cellular ultrastructures at endogenous level for correlated light and electron microscopy (CLEM) or lattice light-sheet microscopy. Overall, the readily and feasible expansion of the methodology will pioneer the non-genetically encoded visualization of cellular networks and subcellular structures and

1 hence provide complementary and unique information at unprecedented precision. Thus,

2 fluorobody delivery by cell squeezing for in-cell tracing will likely find applications supporting

3 routine imaging of multiple native cellular assemblies with advanced imaging techniques.

4

Acknowledgement

12

Authors Contribution

14 A.K. performed the nanobody labeling and cell squeezing experiments. S.H., A.K., and F.T. carried

15 out the protein expression and purification. A.R. and M.H. performed the *d*STORM imaging and

16 analysis. A.K., R.W., and R.T. wrote the manuscript and analyzed the data. R.W. and R.T.

17 conceived the ideas and directed the work.

18

Competing Financial Interests The authors declare no competing financial interests.

20

References

22 1 Schnell, U., Dijk, F., Sjollema, K.A. & Giepmans, B.N. Immunolabeling artifacts and the need for live-
23   cell imaging. *Nat Methods* **9**, 152-158 (2012).
24 2 Cubitt, A.B. *et al.* Understanding, improving and using green fluorescent proteins. *Trends Biochem*
25   *Sci* **20**, 448-455 (1995).
26 3 Gautier, A. *et al.* An engineered protein tag for multiprotein labeling in living cells. *Chem Biol* **15**,
27   128-136 (2008).
28 4 El-Husseini, A.E., Schnell, E., Chetkovich, D.M., Nicoll, R.A. & Bredt, D.S. PSD-95 involvement in
29   maturation of excitatory synapses. *Science* **290**, 1364-1368 (2000).

10

5   Brauchle, M. *et al.* Protein interference applications in cellular and developmental biology using DARPins that recognize GFP and mCherry. *Biol Open* **3**, 1252-1261 (2014).

6   Karatan, E. *et al.* Molecular recognition properties of FN3 monobodies that bind the Src SH3 domain. *Chem Biol* **11**, 835-844 (2004).

7   Nygren, P.A. Alternative binding proteins: affibody binding proteins developed from a small three-helix bundle scaffold. *FEBS J* **275**, 2668-2676 (2008).

8   Skerra, A. Engineered protein scaffolds for molecular recognition. *J Mol Recognit* **13**, 167-187 (2000).

9   Bird, R.E. *et al.* Single-chain antigen-binding proteins. *Science* **242**, 423-426 (1988).

10   Huston, J.S. *et al.* Protein engineering of antibody binding sites: recovery of specific activity in an anti-digoxin single-chain Fv analogue produced in Escherichia coli. *Proc Natl Acad Sci U S A* **85**, 5879-5883 (1988).

11   Muyldermans, S. Single domain camel antibodies: current status. *J Biotechnol* **74**, 277-302 (2001).

12   Helma, J., Cardoso, M.C., Muyldermans, S. & Leonhardt, H. Nanobodies and recombinant binders in cell biology. *J Cell Biol* **209**, 633-644 (2015).

13   Caussinus, E., Kanca, O. & Affolter, M. Fluorescent fusion protein knockout mediated by anti-GFP nanobody. *Nat Struct Mol Biol* **19**, 117-121 (2011).

14   Maier, J., Traenkle, B. & Rothbauer, U. Real-time analysis of epithelial-mesenchymal transition using fluorescent single-domain antibodies. *Sci Rep* **5**, 13402 (2015).

15   Zolghadr, K., Gregor, J., Leonhardt, H. & Rothbauer, U. Case study on live cell apoptosis-assay using lamin-chromobody cell-lines for high-content analysis. *Methods Mol Biol* **911**, 569-575 (2012).

16   Rothbauer, U. *et al.* Targeting and tracing antigens in live cells with fluorescent nanobodies. *Nat Methods* **3**, 887-889 (2006).

17   Schornack, S. *et al.* Protein mislocalization in plant cells using a GFP-binding chromobody. *Plant J* **60**, 744-754 (2009).

18   Tang, J.C. *et al.* Detection and manipulation of live antigen-expressing cells using conditionally stable nanobodies. *eLife* **5** (2016).

19   Plessner, M., Melak, M., Chinchilla, P., Baarlink, C. & Grosse, R. Nuclear F-actin formation and reorganization upon cell spreading. *J Biol Chem* **290**, 11209-11216 (2015).

20   Melak, M., Plessner, M. & Grosse, R. Actin visualization at a glance. *J Cell Sci* **130**, 525-530 (2017).

21   Katrukha, E.A. *et al.* Probing cytoskeletal modulation of passive and active intracellular dynamics using nanobody-functionalized quantum dots. *Nat Commun* **8**, 14772 (2017).

22   Teng, K.W. *et al.* Labeling proteins inside living cells using external fluorophores for microscopy. *eLife* **5** (2016).

23   Kollmannsperger, A. *et al.* Live-cell protein labelling with nanometre precision by cell squeezing. *Nat Commun* **7**, 10372 (2016).

24   Sharei, A. *et al.* A vector-free microfluidic platform for intracellular delivery. *Proc Natl Acad Sci U S A* **110**, 2082-2087 (2013).

25   Ries, J., Kaplan, C., Platonova, E., Eghlidi, H. & Ewers, H. A simple, versatile method for GFP-based super-resolution microscopy via nanobodies. *Nat Methods* **9**, 582-584 (2012).

26   Kirchhofer, A. *et al.* Modulation of protein properties in living cells using nanobodies. *Nat Struct Mol Biol* **17**, 133-138 (2010).

27   Pleiner, T. *et al.* Nanobodies: site-specific labeling for super-resolution imaging, rapid epitope-mapping and native protein complex isolation. *eLife* **4**, e11349 (2015).

28   Heilemann, M. *et al.* Subdiffraction-resolution fluorescence imaging with conventional fluorescent probes. *Angew Chem Int Ed Engl* **47**, 6172-6176 (2008).

1 **Methods**

2

3 **Plasmid construction**

4 For expression in *E. coli*, the α-GFP nanobody,[26] equipped with a C-terminal His$_6$-tag for

5 purification via metal ion affinity chromatography, was inserted into the pET21a(+) plasmid. For

6 site-specific labeling, a free single cysteine was introduced C-terminally to the His$_6$-tag. The α-GFP

7 nanobody was PCR amplified by the following primers: fw 5'-GCGCGC<u>AAGCTT</u>*AAGG*

8 *AG*ATATACAT**ATG**CAGGTTCAGCTGGTTGAAAGCGGTGGTGCAC-3' (Hind III restriction site

9 underlined, RBS italic, start codon bold); rev 5'-GCGC<u>CTCGAG</u>G**TCAGCA***GTGGTGATGG*

10 *TGATGATG*GCTGCTAACGGTAACCTGGGTGCCC-3' (XhoI restriction site underlined, stop

11 codon bold, cysteine bold and underlined, His$_6$-tag italic). For expression in mammalian cells,

12 α-GFP as well as mCherry were PCR amplified and introduced into the pcDNA3.1(+) plasmid,

13 resulting in a plasmid coding for α-GFP^{mCherry}. fw 5'-GCGCGC<u>GCTAGC</u>ACC**ATG**CAGGTTCA

14 GCTGGTTGAAAGCGG-3' (NheI restriction site underlined, start codon bold) and rev

15 5'-GCGCGC<u>GGTACC</u>GCTGCTAACGGTAACCTGGGTGCCC-3' (Acc65I restriction site

16 underlined) for the α-GFP nanobody and fw 5'-CGCGC<u>GGTACC</u>**ATG**GTGAGCAAGGGCGAG

17 GAGCTGTTC-3' (Acc65I restriction site underlined, start codon bold) and rev

18 5'-GCGCGC<u>CTCGAG</u>**TTA**CTTGTACAGCTCGTCCATGCCGAGAG-3' (XhoI restriction site

19 underlined, stop codon bold) for mCherry. The α-Lamin nanobody was also inserted into the

20 pET21a(+) plasmid and equipped with a His$_6$-tag for purification. Using α-Lamin-EGFP as PCR

21 template, α-Lamin was amplified, introducing a C-terminal cysteine (α-Lamin$^{His6-Cys}$), a N-terminal

22 cysteine (^{Cys}α-Lamin^{His6}), or replacing serine 9 by a cysteine (α-Lamin$^{S9C-His6}$). α-Lamin$^{His6-Cys}$:

23 fw 5'-GCGC<u>AAGCTT</u>*AAGGAGA*TATACAT**ATG**GCTCAGGTACAGCTGCAGGAGTCTGGAGGA

24 GG-3' (HindIII restriction site underlined, start codon bold, RBS italic); rev 5'-GCGC<u>CTCGAG</u>

25 **TTA**<u>**ACA**</u>*GTGGTGATGGTGATGATG*CGATATCGAATTCCTTGAGGAGACGGTGACCTGGG-3'

26 (XhoI restriction site underlined, stop codon bold, cysteine bold and underlined, His$_6$-tag italic).

1   To attach the PelB leader sequence and the cysteine, ^{Cys}α-Lamin^{His6} were amplified in consecutive

2   extending PCRs, each of them being the template for the subsequent amplification. The rev primer

3   5'-GCGCGC<u>CTCGAG</u>**TTA***GTGGTGATGGTGATGATG*GGTGGCGACCGGCCG-3'   (XhoI

4   restriction site underlined, stop codon bold, His$_6$-tag italic) was thereby applied in combination with

5   the following fw primers. ^{Cys}α-Lamin^{His6}: fw1 5'-*GGATTGTTATTACTCGCGGC*

6   *CCAGCCGGCC***TGT**GCTCAGGTACAGCTGCAGGAGTCTGGAGGAGG-3' (cysteine bold, part

7   of pelB leader sequence italic), fw2 5'-GCGC<u>GCTAGC</u>**ATG***AAATACCTATTGCCTACGGCAG*

8   *CCGCTGGATTGTTATTACTCGCGGCCCAGCCGGCC*-3' (NheI restriction site underlined, start

9   codon bold, pelB leader sequence italic). α-Lamin$^{S9C-His6}$: fw1 5'-ATGGCTCAGGTACAGCTGC

10   AGGAGTGTGGAGGAGGCTTGGTGCAGGCAGGGGGGTCTCTG-3', fw2 5'-*GGATTGTTAT*

11   *TACTCGCGGCCCAGCCGGCC*ATG GCTCAGGTACAGCTGCAGGAG**TGT**GGA-3' (cysteine

12   bold, part of pelB leader sequence italic), fw3 5'-GCGC<u>GCTAGC</u>**ATG***AAATACCTATT*

13   *GCCTACGGCAGCCGCTGGATTGTTATTACTCGCGGCCCAGCCGGCC*-3' (NheI restriction site

14   underlined, start codon bold, pelB leader sequence italic). The plasmid coding for H2B-EGFP was

15   obtained from Addgene (plasmid 11680). The generation of plasmids coding for core TAP1 (TAP1-

16   mVenus) and mEGFP-Lamin A was described previously.[23,29]

17

18   **Nanobody production**

19   The nanobodies were produced in *E. coli* BL21 (DE3, Life technologies) or *E. coli* SHuffle T7

20   Express (New England Biolabs), whereas the latter contains a chromosomal copy of a disulfide

21   isomerase, engineered to produce proteins with disulfide bonds in the cytosol. Both *E. coli* strains

22   were transformed with the vectors, coding for α-GFP and α-Lamin nanobodies with engineered

23   cysteines. A single colony was inoculated in LB medium containing 100 µg/ml ampicillin and

24   2% (w/v) glucose. After overnight incubation (37 °C for *E. coli* BL21 (DE3) and 30 °C for *E. coli*

25   SHuffle T7 Express, 180 rpm), 1 l Lysogeny Broth (LB) medium with 100 µg/ml ampicillin was

26   inoculated and protein expression was induced at A$_{600}$ of 0.7-0.8 by 1 mM isopropyl-β-

1 thiogalactopyranoside (IPTG, Sigma-Aldrich) and conducted for 5-20 h (30 °C, 180 rpm). After

2 centrifugation (20 min, 4°C, 5,000x g), the cell pellets were directly used for protein purification or

3 stored at -20 °C.

4

5 **Protein purification**

6 Two different protocols were used for purification. For α-GFP[His6-Cys] and α-Lamin[His6-Cys] expressed

7 in *E. coli* BL21 (DE3), cell pellets were resuspended in lysis buffer (20 mM Tris pH 8.0,

8 100 mM NaCl, 1 mM phenylmethylsulfonyl fluoride (PMSF), 0.5 mM β-mercaptoethanol (β-ME)),

9 followed by sonication for cell lysis. Cell debris were pelleted by ultracentrifugation (100,000x g,

10 30 min, 4 °C). For metal affinity chromatography, the supernatant was incubated with 3 ml Ni-NTA

11 Sepharose beads (GE Healthcare) in the presence of imidazole (15 mM). Afterwards, the beads

12 were washed in purification buffer (50 mM Tris pH 8.0, 300 mM NaCl, 50 mM imidazole, 0.5 mM

13 β-ME). His-tagged proteins were eluted by 200 mM imidazole/purification buffer. Protein

14 concentration was determined at A_{280}. Buffer exchange to phosphate-buffered saline (PBS)

15 containing 0.5 mM β-ME by Zeba spin desalting columns (7K) was followed by concentration via

16 Amicon Ultra Filters (3 K). β-ME was directly removed before labeling the nanobodies using Zeba

17 spin desalting columns (7K). Alternatively, nanobodies expressed in *E. coli* T7 Express were

18 purified as described above, but at pH 7.5 and without β-ME.

19

20 **Protein modification**

21 Fluorescent dyes were either attached to the engineered cysteines or to lysines (only for

22 α-Lamin[His6-Cys]). The engineered cysteines of nanobodies stored in PBS without β-ME were

23 reduced by incubation with 15 mM TCEP for 10 min on ice and subsequent buffer exchange by

24 Zeba spin desalting columns (7K). Cysteine labeling was conducted following two different

25 protocols. On the one hand, nanobodies were incubated with sulfo-Cy5 (sCy5) or sulfo-Cy3 (sCy3)

14

1 maleimide in PBS (pH 7.4) for 1.5 h at 4 °C. Labeling was conducted at a protein concentration of

2 approximately 1 mg/ml with 1.2-fold molar excess of the dye. For the alternative labeling protocol,

3 buffer was exchanged to maleimide labeling buffer after TCEP reduction (100 mM KH_2PO_4 pH 6.4,

4 150 mM NaCl, 1 mM EDTA, 250 mM sucrose). Afterwards, the fluorophore was added in a 1.2-

5 fold molar excess, immediately followed by neutralization to pH 7.5 using K_2HPO_4 and 1.5 h

6 incubation at 4 °C. For lysine labeling, nanobodies in PBS (pH 7.4) were mixed 1:20 with 0.1 mM

7 $NaHCO_3$ (pH 9.0) to achieve pH 8.3 for labeling. Next, Alexa647 NHS ester was added with a

8 5-fold molar excess. Labeling was performed for 1 h at 20 °C before buffer exchange and removal

9 of excess dye with Zeba spin desalting columns (7K, Thermo Scientific). Fluorescently labeled

10 nanobodies were analyzed by SDS-PAGE and in-gel fluorescence (Typhoon 9400 Imager; $\lambda_{ex/em}$

11 630/670 nm). Fbs were finally purified by size-exclusion chromatography in PBS using a

12 KW404-4F column (Shodex; flow rate 0.3 ml/min). All labeled nanobodies were stored in PBS at

13 4 °C. The nanobody-to-fluorophore ratio was determined using absorption (A_{280} for nanobodies,

14 A_{550} for sCy3, A_{663} for ATTO655, A_{649} for sCy5) and their respective extinction coefficient

15 ε ($0.22 \cdot 10^5$ $M^{-1} \cdot cm^{-1}$ for α-Lamin Nb, $0.27 \cdot 10^5$ $M^{-1} \cdot cm^{-1}$ for α-GFP Nb, $1.36 \cdot 10^5$ $M^{-1} \cdot cm^{-1}$ for sCy3,

16 $1.25 \cdot 10^5$ $M^{-1} \cdot cm^{-1}$ for ATTO655, and $2.50 \cdot 10^5$ $M^{-1} \cdot cm^{-1}$ for sCy5).

17

18 **Cell culture and transfection**

19 HeLa Kyoto cell lines were cultivated in Dulbecco's Modified Eagle Medium (DMEM) with 4.5 g/l

20 glucose (Gibco) containing 10% (v/v) fetal calf serum (FCS, Gibco). Cells were regularly tested

21 for Mycoplasma contamination.[30] Cells were transiently transfected using Lipofectamine 2000

22 (Life technologies), following the manufacturer's instructions. For staining of fixed cells, $2 \cdot 10^4$ cells

23 per well were seeded into 8-well on cover glass II slides (Sarstedt) and transfected at ~ 80%

24 confluency. For cell squeezing, $8 \cdot 10^5$ cells were seeded into 6-well cell culture plates (Greiner)

25 and transiently transfected. After transfection, cells were incubated for 12-24 h at standard cell

26 culture conditions until experiments were performed.

1   Cell fixation and labeling

2   Cells were washed with PBS (Sigma-Aldrich), fixed with 4% formaldehyde (Roth)/PBS for

3   10-20 min at 20 °C and permeabilized using 0.1% Triton X-100 (Roth)/PBS (10 min, 20 °C). After

4   blocking with 5% (w/v) bovine serum albumin (BSA; Albumin Fraction V, Roth) in PBS for 1 h at

5   20 °C, cells were stained. Staining was performed with fluorobodies (diluted in 1% BSA/PBS) at

6   concentrations ranging from 50 to 500 nM (indicated in each case). Subsequently, cells were

7   washed with PBS and optionally stained with 0.1 µg/ml 4',6-diamidino-2-phenylindole (DAPI,

8   Sigma-Aldrich) in 1% BSA/PBS for 30 min to 1 h at 20 °C. After washing with 5% BSA/PBS (3x),

9   cells were post-fixed with 2% formaldehyde/PBS (15 min, 20 °C) and stored in PBS until imaging

10   was performed.

11

12   Confocal laser scanning microscopy

13   Imaging was performed using the confocal laser scanning (LSM) microscope LSM880 (Zeiss) or

14   TCS SP5 microscope (Leica) with Plan-Apochromat 63x/1.4 Oil DIC objectives. To avoid crosstalk

15   between different fluorophores, images were acquired sequentially. The following laser lines were

16   used for excitation: 405 nm for DAPI; 488 nm for EGFP, mEGFP, and mVenus; 565 nm for sCy3;

17   633 nm for sCy5 and ATTO655. Live-cell imaging of endogenous proteins (except for dual-color

18   imaging with ATTO488 and ATTO655) was conducted with the Airy scan detector of the LSM880

19   in the SR-mode. For 3D reconstructions of labeled protein networks, z-stack were recorded with

20   the Airy scan detector (distance between stacks ~ 200 nm). For live-cell imaging, an incubation

21   system was used to keep cells at 37 °C and supply them with 5% CO_2 during imaging. ImageJ[31],

22   Fiji[32], and Zen 2.3 black (Zeiss) were used for image analysis and to analyze Pearson's

23   coefficients from 8-11 individual cells per condition. The mean and standard deviation were

24   calculated.

25

Fluorobody transfer by cell squeezing

Squeezing was performed using a chip with constrictions of 7 µm in diameter and 10 µm in length (CellSqueeze 10-(7)x1, SQZbiotech). In all microfluidic experiments, a cell density of $1.5 \cdot 10^6$ cells/ml in 10% (v/v) FCS/PBS was squeezed through the chip at a pressure of 30 psi. Transduction was conducted at 4 °C to block cargo uptake by endocytosis.[23] During squeezing, the following Fb concentrations in the surrounding buffer were used: 100-200 nM of α-GFP, 200-500 nM of α-Lamin, and 50 µg/ml of α-Vimentin. After squeezing, cells were incubated for 5 min at 4 °C to reseal the plasma membrane. Squeezed cells were washed with DMEM containing 10% FCS, seeded into 8-well on cover glass II slides (Sarstedt) or collagen-coated dishes (µ-Slide 8 Well, Collagen IV coverslip, ibidi) in DMEM containing 10% FCS, and cultured at 37 °C and 5% CO_2. Confocal imaging was performed 1 h and 20 h after squeezing. Squeezing experiments for live-cell protein labeling highly reproducible in at least three independent experiments for every POI.

Super-resolution microscopy

For super-resolution imaging of the α-Lamin[ATTO655] Fb in live cells, a custom-built microscope was used. Samples were illuminated with 643 nm (iBeam smart, Toptica Photonics) laser beams and a 405 nm reactivation laser (Cube 405-50C, Coherent) in total internal reflection fluorescence (TIRF) mode. The excitation light was focused on the back focal plane of a 100x oil objective (Plan Apo 100x TIRFM, NA 1.45, Olympus), mounted on an inverted microscope (Olympus IX71). The emission was recorded using an EMCCD camera (IxonUltra, Andor) with frame-transfer mode, 1x pre-amplifier gain and EM gain set to 200. For every sample, 40,000 images were recorded at a frame rate of 33 Hz. Image reconstruction was performed with rapidSTORM[33] using the smooth by differences of averages option with a signal-to-noise ratio of 20, fitting only PSFs with FWHM ranging from 240-520 nm and X-Y-ratio of 0.7-1.3. The average localization precision (σ_{loc}) defined as the nearest neighbor distance in adjacent frames[34] was calculated to 23.4 ± 8.3 nm for living

1 and 23.2 ± 4.6 nm for fixed cells (mean and standard deviation of three individually analyzed cells,

2 respectively) using LAMA software.[35] The average image used for visualization of nuclear

3 intensity profiles in Figure 3f was generated by averaging the fluorescence intensity over 100

4 frames and subsequent background subtraction with a rolling ball method (20 pixel radius) in

5 ImageJ and Fiji.

6

Data availability

8 The datasets generated during and/or analyzed during the current study are available from the

9 corresponding author on reasonable request.

10

Supplementary References

12 23 Kollmannsperger, A. *et al.* Live-cell protein labelling with nanometre precision by cell squeezing. *Nat*
13 *Commun* **7**, 10372 (2016).
14 26 Kirchhofer, A. *et al.* Modulation of protein properties in living cells using nanobodies. *Nat Struct Mol*
15 *Biol* **17**, 133-138 (2010).
16 29 Parcej, D., Guntrum, R., Schmidt, S., Hinz, A. & Tampé, R. Multicolour fluorescence-detection size-
17 exclusion chromatography for structural genomics of membrane multiprotein complexes. *PLoS One*
18 **8**, e67112 (2013).
19 30 Uphoff, C.C. & Drexler, H.G. Detection of mycoplasma contamination in cell cultures. *Curr Protoc*
20 *Mol Biol* **106**, 28 24 21-28 24 14 (2014).
21 31 Girish, V. & Vijayalakshmi, A. Affordable image analysis using NIH Image/ImageJ. *Indian J Cancer* **41**,
22 47 (2004).
23 32 Schindelin, J. *et al.* Fiji: an open-source platform for biological-image analysis. *Nat Methods* **9**, 676-
24 682 (2012).
25 33 Wolter, S. *et al.* Real-time computation of subdiffraction-resolution fluorescence images. *J Microsc*
26 **237**, 12-22 (2010).
27 34 Endesfelder, U., Malkusch, S., Fricke, F. & Heilemann, M. A simple method to estimate the average
28 localization precision of a single-molecule localization microscopy experiment. *Histochem Cell Biol*
29 **141**, 629-638 (2014).
30 35 Malkusch, S. & Heilemann, M. Extracting quantitative information from single-molecule super-
31 resolution imaging data with LAMA - LocAlization Microscopy Analyzer. *Sci Rep* **6**, 34486 (2016).

32

33
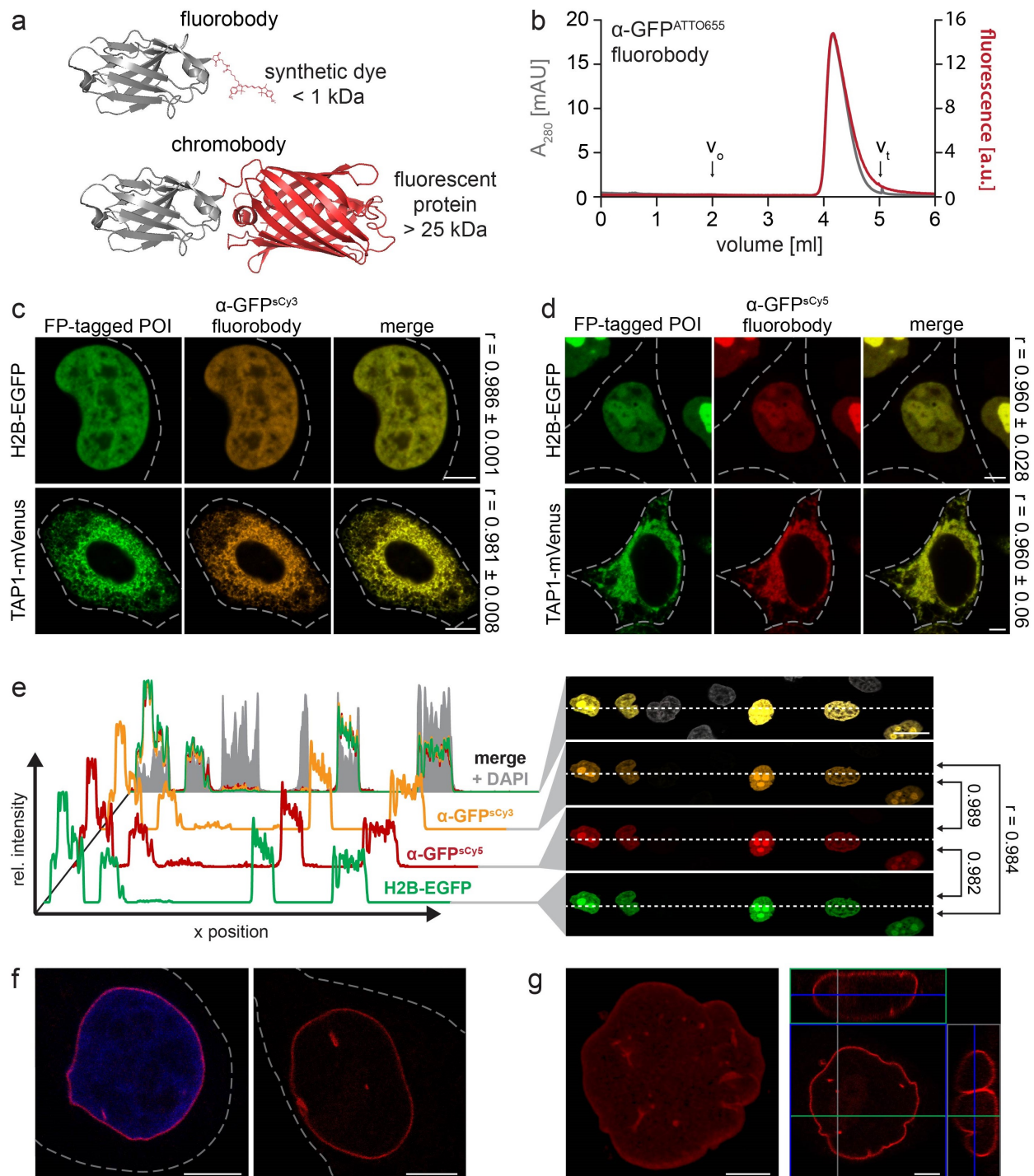
Figures

Figure 1 I Specific binding of site-specifically labeled fluorobodies. (**a**) Size comparison of nanobodies labeled with a fluorescent protein (chromobody) or a synthetic dye (fluorobody). Bulky fluorescent proteins (> 25 kDa) triple the size of the nanobody (~13 kDa). In comparison, the

1   minimal size of fluorophores (< 1 kDa) is unlikely to disturb the nanobody and offer a higher

2   quantum yield as well as photostability. mCherry (PDB 2H5Q) is shown exemplarily. (**b**) Size-

3   exclusion chromatography (SEC) of the site-specifically labeled α-GFP^{ATTO655} Fb. The grey and

4   red lines represent absorption at 280 nm (A$_{280}$) and ATTO655 fluorescence at $\lambda_{ex/em}$ 655/680 nm.

5   Chromatogram shows specific modification of the nanobody and high purity. (**c**, **d**) Specific

6   labeling of FP-tagged proteins in chemically arrested cells. HeLa Kyoto cells expressing

7   H2B-EGFP or TAP1-mVenus (green) were fixed with 4% formaldehyde and labeled with 100 nM

8   of α-GFP^{sCy3} (**c**, orange) or α-GFP^{sCy5} (**d**, red) Fb. Excellent co-localization (merge) between the

9   Fbs and both FP-tagged POIs was detected. Pearson's coefficients (r) were calculated from 9-11

10   individual cells (right). (**e**) Fixed HeLa Kyoto cells expressing H2B-EGFP were stained with

11   α-GFP^{sCy3} (orange), α-GFP^{sCy5} (red, 100 nM each), and DAPI (blue). Cross-sections of relative

12   fluorescence intensity profiles of both Fbs (along dashed line) highly correlated with the expression

13   level of H2B-EGFP. Low background fluorescence was detected in untransfected cells (only DAPI

14   positive), supported by the Pearson's coefficients (r) between different channels (right). (**f**, **g**) After

15   fixation, the endogenous nuclear lamina of HeLa Kyoto cells was visualized by 100 nM of

16   α-Lamin^{ATTO655} Fb (red). (**g**) The Fb specifically decorated the nuclear envelope (DNA optionally

17   visualized via DAPI staining, blue). (**f**) 3D reconstruction of a z-stack showed a dense labeling of

18   the nuclear lamina along with a high signal-to-background ratio (see Supplementary Video 1).

19   Images were taken by CLSM with the Airy Scan detector (f and g). Dashed lines indicate the cell

20   border. Scale bars: 5 μm (**c**,**d**,**f**,**g**) and 20 μm (**e**).
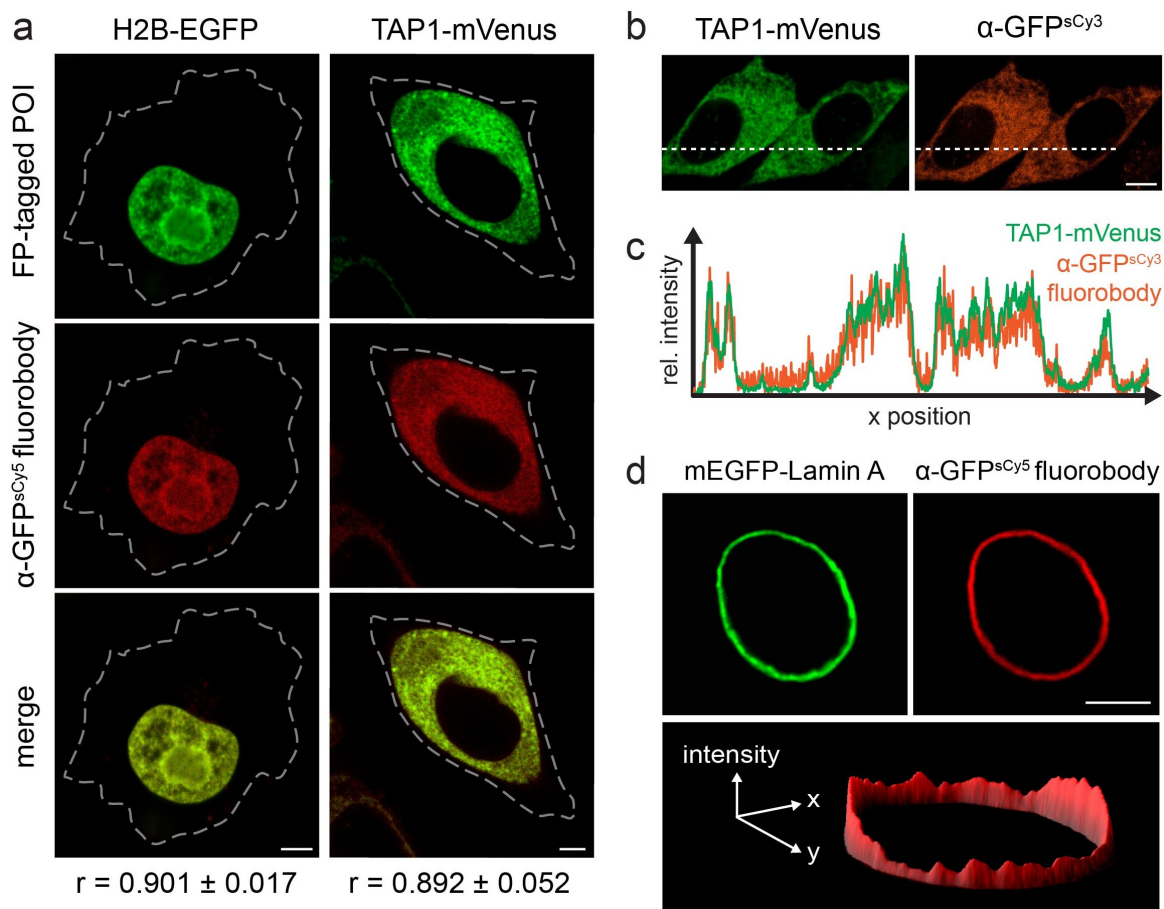
Figure 2 I Live-cell protein labeling with high-performance fluorobodies. (**a**) Protein labeling in living cells at different subcellular localizations. The α-GFP^{sCy5} Fb (200 nM, red) was delivered via cell squeezing into HeLa Kyoto cells, expressing H2B-EGFP or TAP1-mVenus (green). Excellent co-localization (merge channel) of the Fbs with both FP-tagged POIs was observed 3 h post squeezing by CLSM. The Pearson's coefficients (r, bottom) ranging from 0.864 to 0.905 were calculated from 8-10 individual cells. Dashed lines indicate cell borders. (**b**) Live-cell visualization of TAP1-mVenus (green) by α-GFP^{sCy3} Fb (orange) 20 h after squeezing. Cross-sections of relative fluorescence intensity profiles of TAP1-mVenus and α-GFP^{sCy3} (along dashed line) showed specific and low-background labeling in live cells by the α-GFP Fb (**c**). Pearson's coefficient: 0.926. (**d**) 3D intensity plot of a representative HeLa Kyoto cell expressing mEGFP-Lamin A (green) was stained by α-GFP^{sCy5} Fb (red) and showed a very high signal-to background ratio. All images were taken by CLSM. Scale bar: 5 μm.

21

1
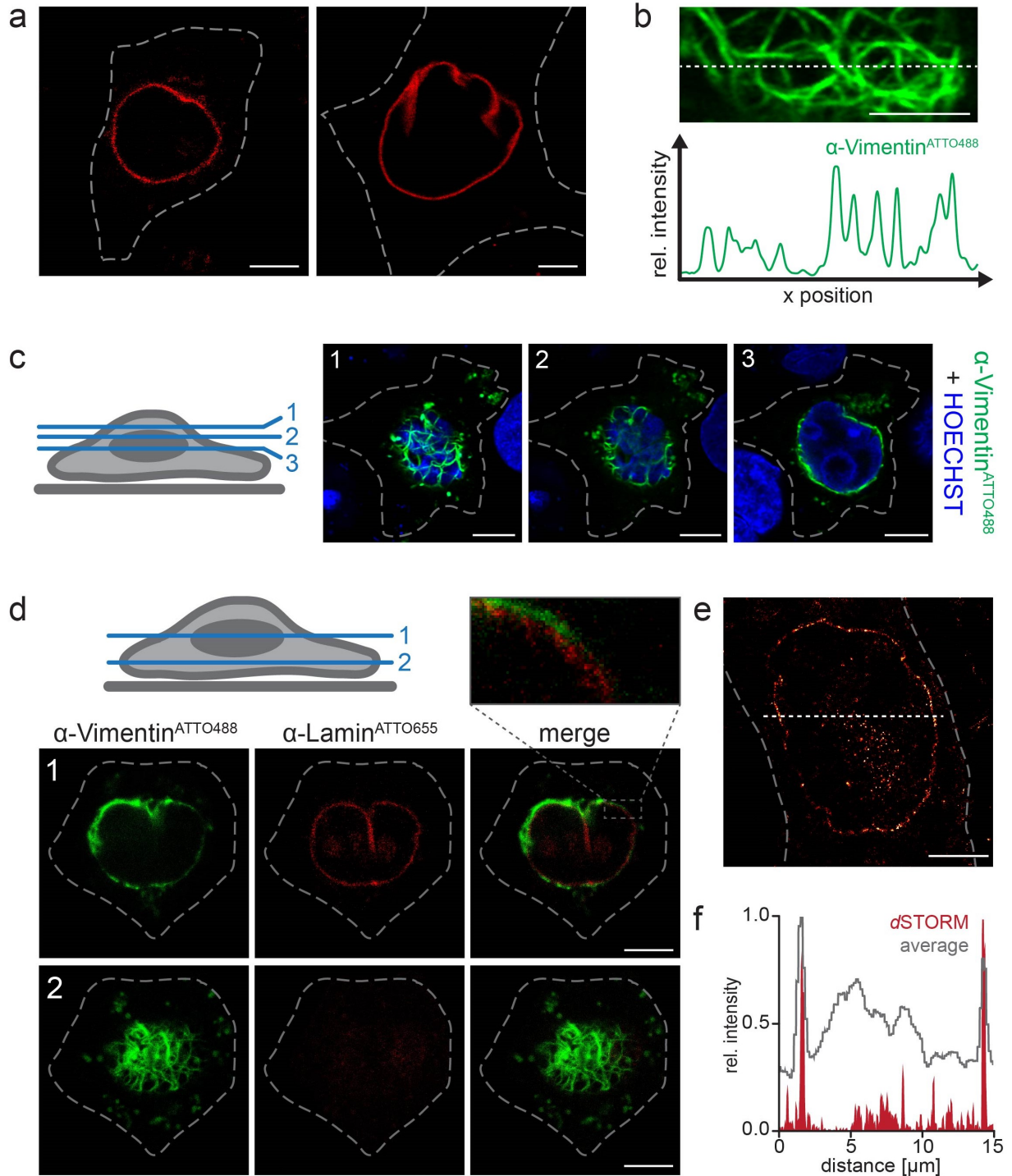
Figure 3 l Dual-color live-cell tracing of endogenous targets and live-cell super-resolution imaging by fluorobodies. (**a**) The α-Lamin[ATTO655] Fb (200 nM) was transferred into HeLa Kyoto cells via squeezing. Confocal imaging after 3 h showed specific labeling of the native nuclear lamina in living cells with high signal-to-background ratio. (**b**) HeLa Kyoto cells were squeezed with 50 µg/ml

1   of α-Vimentin^{ATTO488}. The Fb decorated vimentin network was explicitly traced 3 h post squeezing

2   and visualized as a dense meshwork around the nucleus (HOECHST-positive, blue) in different

3   confocal z-planes (1-3; indicated in scheme, left). (**c**) Fluorescence intensity cross-section of a live

4   HeLa Kyoto cell transduced with α-Vimentin^{ATTO488} (along dashed line) showed specific and distinct

5   decoration of the endogenous vimentin meshwork with high signal-to-background ratio. The

6   respective network was localized beneath the nucleus (corresponding to z-plane 2 in d). (**d**) Dual-

7   color labeling of endogenous lamin and vimentin in living cells. α-Lamin^{ATTO655} and

8   α-Vimentin^{ATTO488} were simultaneously transferred into HeLa Kyoto cells. 3 h after cell squeezing,

9   spatially distinct labeling of endogenous lamin (red) and vimentin (green) was visualized by

10   multiplexed imaging. Magnification (box, top) of the α-Vimentin^{ATTO488} stained vimentin network

11   showed the three-dimensional organization around the nucleus. The respective confocal z-planes

12   are indicated in the scheme. (**e**) Reconstructed *d*STORM image of endogenous lamin specifically

13   labeled with α-Lamin^{ATTO655} Fb (5 h after squeezing). The sensitive and high degree of Fb labeling

14   allowed for visualization of the native nuclear envelope with nanometer precision. (**f**) Comparison

15   of *d*STORM analysis with the averaged fluorescence intensity. Cross section of the intensity

16   profiles (along dashed line in e) displayed the enhanced resolution by *d*STROM. Images were

17   taken by CLSM (a-d) with the Airy detector (except for d) or *d*STORM (e). Dashed lines indicate

18   the cell border. Scale bars: 5 μm.

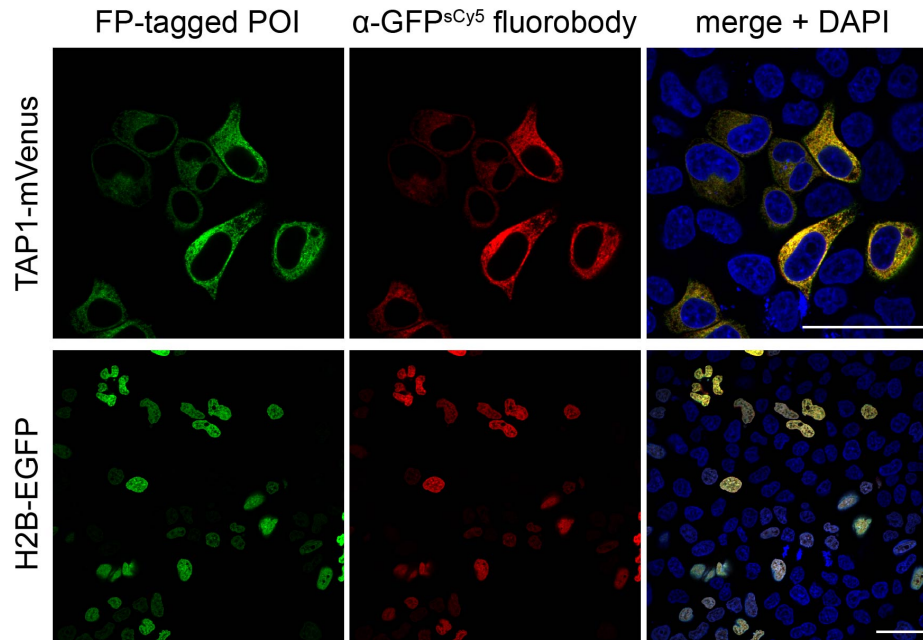1 **SUPPLEMENTAL FIGURES**

InstantBlue™   In-gel fluorescence
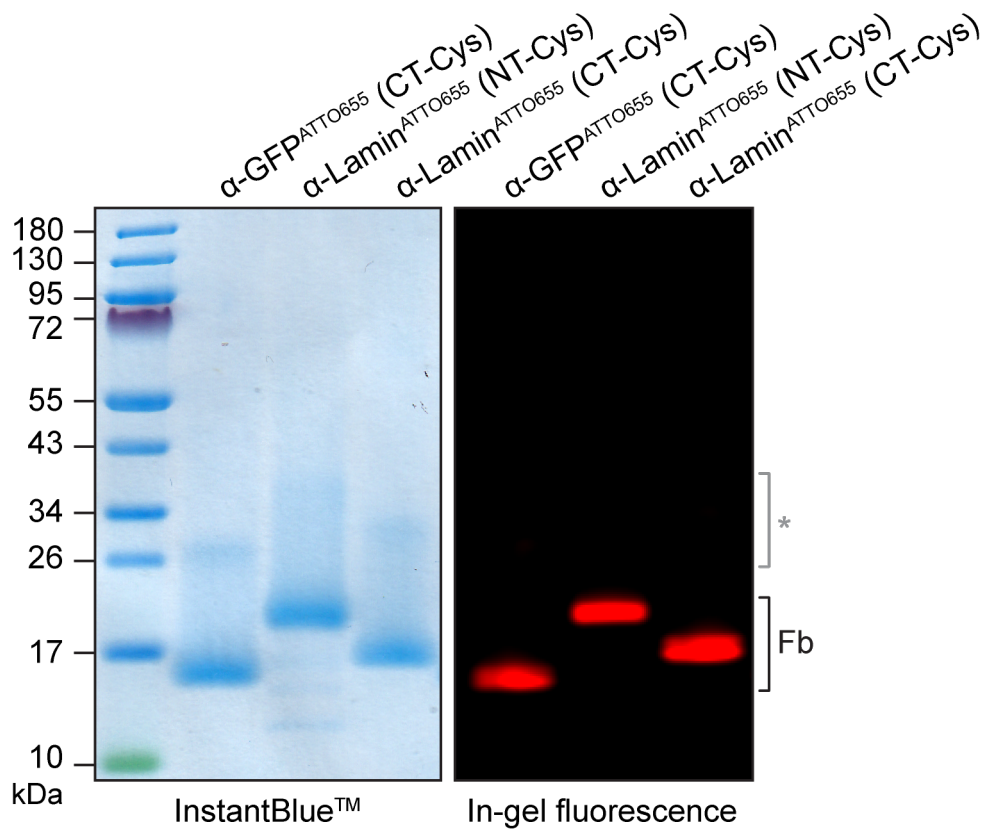
2

3 **Figure 1 – Figure Supplement 1 I Site-specific fluorescent labeling of nanobodies.** Single

4 engineered surface cysteines of nanobodies were modified with maleimide ATTO655. SDS-PAGE

5 analysis showed covalent labeling of the engineered Fbs. Detection was performed by

6 InstantBlue^TM staining and by in-gel fluorescence with $\lambda_{ex/em}$ 630/670 nm. A minor portion of Fb

7 dimers (*) was observed. The higher molecular weight of α-Lamin (NT-Cys) is due to an elongated

8 linker between Nb and C-terminal His$_6$-tag.
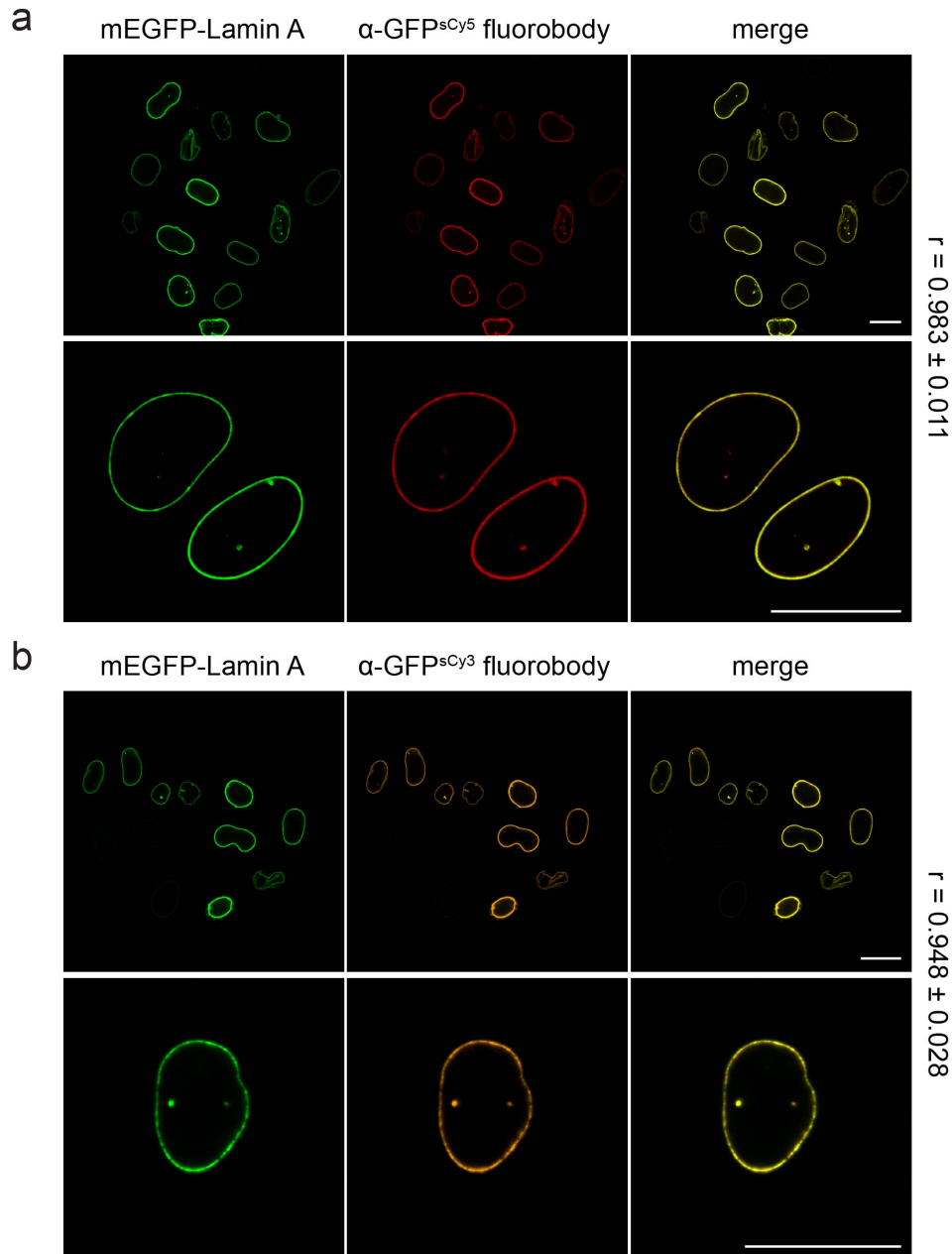
Figure 1 – Figure Supplement 2 I Specific labeling of mEGFP-Lamin A with α-GFP^{sCy3} and α-GFP^{sCy5} fluorobodies. After fixation and permeabilization, HeLa Kyoto cells expressing mEGFP-Lamin A were labeled with 100 nM of α-GFP^{sCy5} Fb (**a**) or α-GFP^{sCy3} Fb (**b**) and analyzed *via* CLSM. mEGFP-Lamin A was specifically labeled by the Fbs with very low background and the staining intensity correlated with the POI´s expression level. Scale bars: 20 µm.

Figure 1 – Figure Supplement 3 I Correlation of the target protein expression level with the labeling density of the α-GFP fluorobody. After fixation and permeabilization, HeLa Kyoto cells expressing TAP1-mVenus or H2B-EGFP were stained with α-GFP^{sCy5} Fb (50 nM). The labeling intensity highly correlates with the expression level of both FP-fused POIs, reflecting stoichiometric target decoration. Imaging was performed by CLSM. Scale bars: 50 μm.
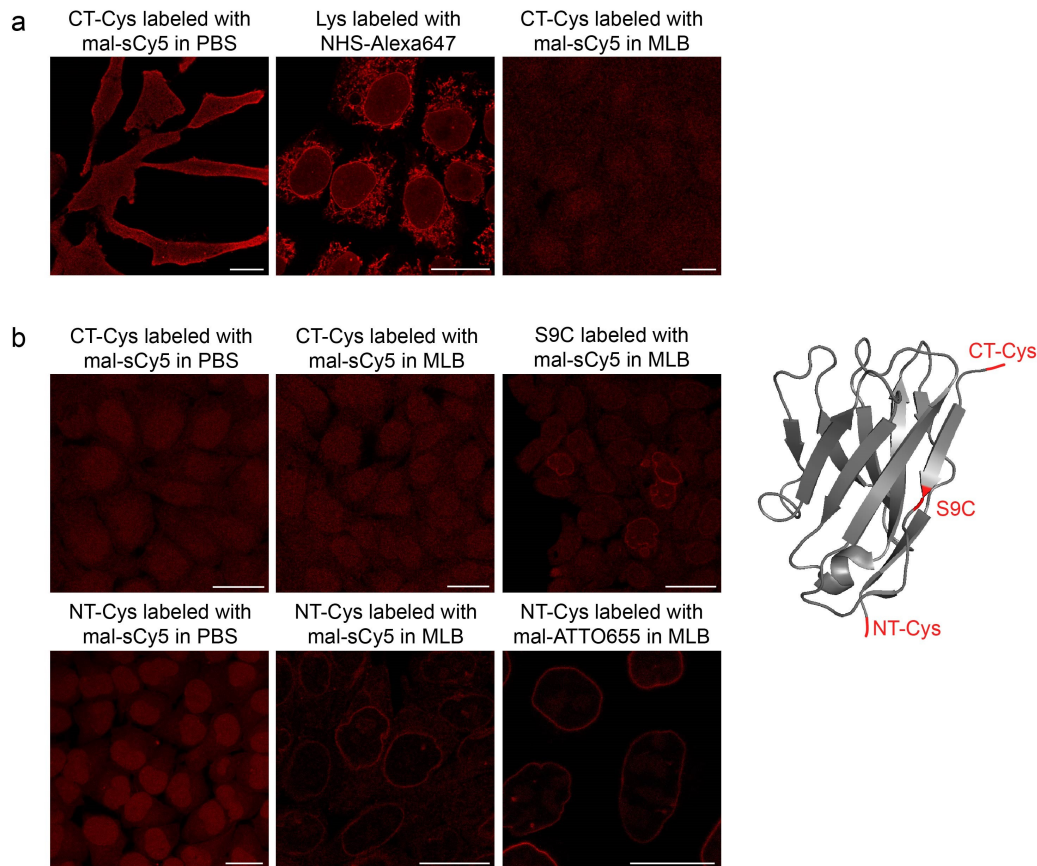
Figure 1 – Figure Supplement 4 I Labeling screen of differently modified α-Lamin fluorobodies. The α-Lamin nanobody was engineered with an extra single cysteine at three different positions, *e.g.* N-terminally (NT-Cys), C-terminally (CT-Cys), or at position 9 (S9C). After production in *E. coli* BL21/DE3 (**a**) or *E. coli* T7 SHuffle Express (**b**) and affinity purification, the engineered nanobodies were modified with maleimide sCy5 or ATTO655. Stochastic labeling via lysines exposed on the nanobody surface was conducted with NHS Alexa647. The specificity of these Fbs was evaluated by staining of HeLa Kyoto cells (500 nM) after fixation and permeabilization. Fb target specificity was analyzed by CLSM. For the CT-Cys labeled, S9C labeled and Lys labeled Fbs a severe lack in target specificity was observed. After production in *E. coli* T7 SHuffle Express and subsequent modification of the N-terminal cysteine in maleimide labeling buffer (MLB), specific tracing of endogenous lamin was achieved with greatly enhanced signal-to-background ratio. This Fb format was used for all further experiments. Scale bars: 20 μm.

1
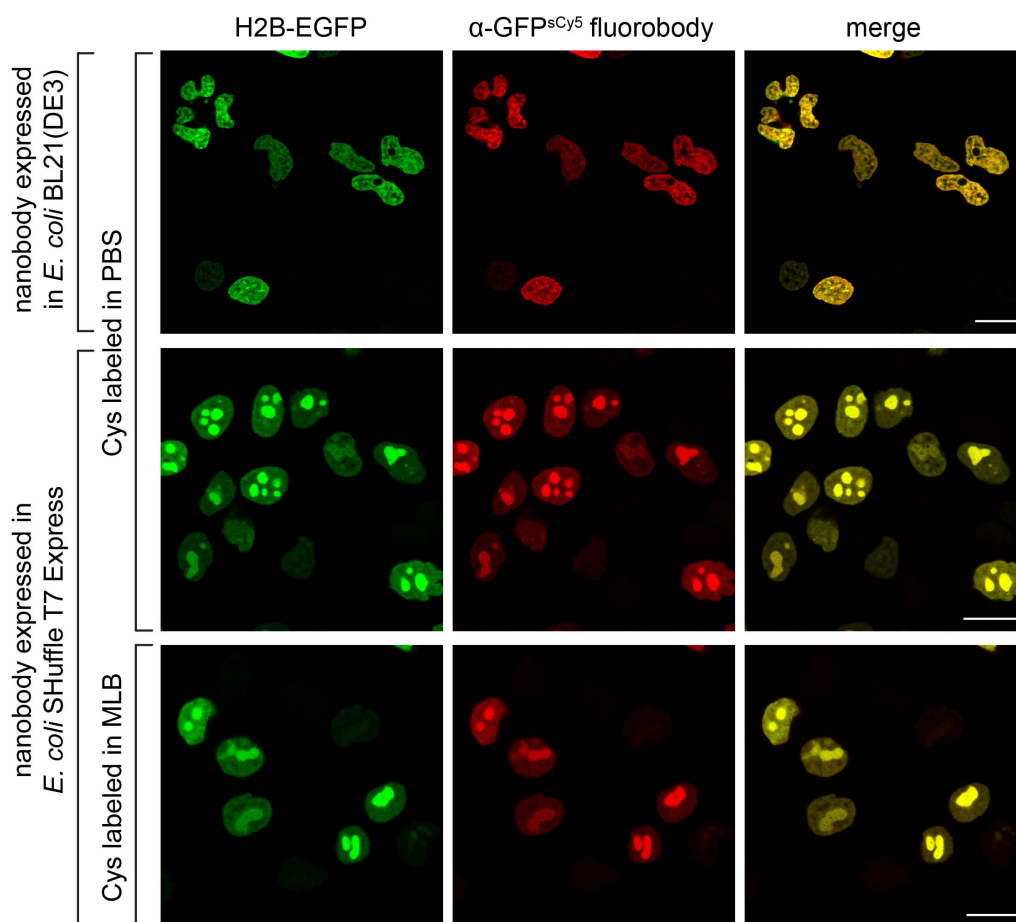
Figure 1 – Figure Supplement 5 | Labeling screen of differently prepared α-GFP fluorobodies. The α-GFP^{sCy5} Fb with an N-terminal cysteine was produced in two different *E. coli* strains (BL21/DE3 or T7 SHuffle Express), and modified with maleimide sCy5. α-GFP binding screen was performed against H2B-EGFP (green) for all tested Fb preparation conditions. Fixed and permeabilized HeLa Kyoto cells were stained with α-GFP^{sCy5} Fb (100 nM, red). All combinations for Fb generation resulted in specific labeling of EGFP-tagged H2B (merge) by the engineered α-GFP with low background labeling. Analysis was performed by CLSM. Scale bars: 20 μm.

1
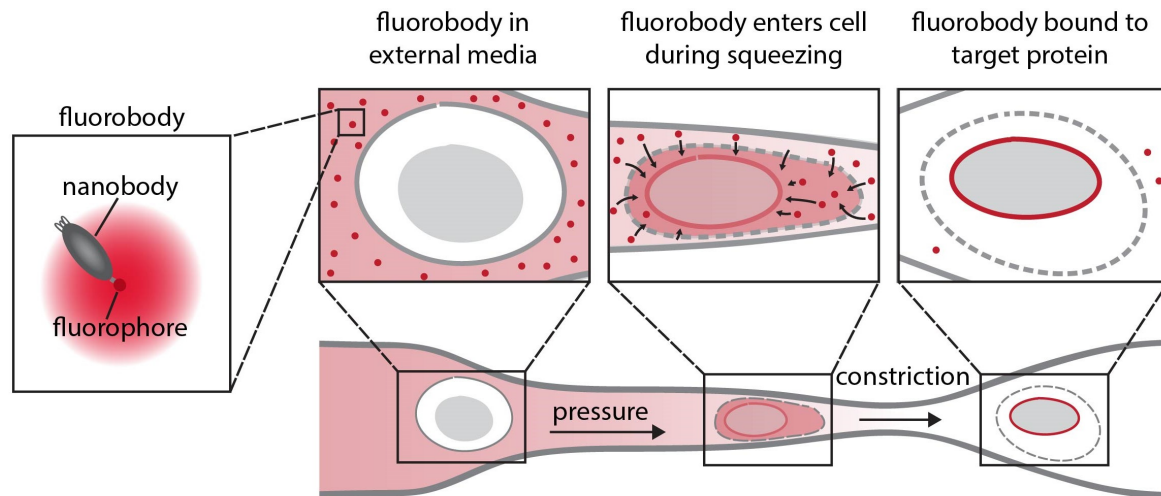
Figure 2 – Supplement Figure 1 I Fluorobody transfer into living cells by microfluidic cell squeezing. Cells are pressed through constrictions, which are ~ 30% smaller than cell diameter. Shear forces cause the formation of transient holes in the plasma membrane. By passive diffusion (middle), site-specifically labeled Fbs enter the cytosol and bind to their target (right, binding to nuclear envelope is exemplarily illustrated). The induced holes reseal within ~ 5 min.
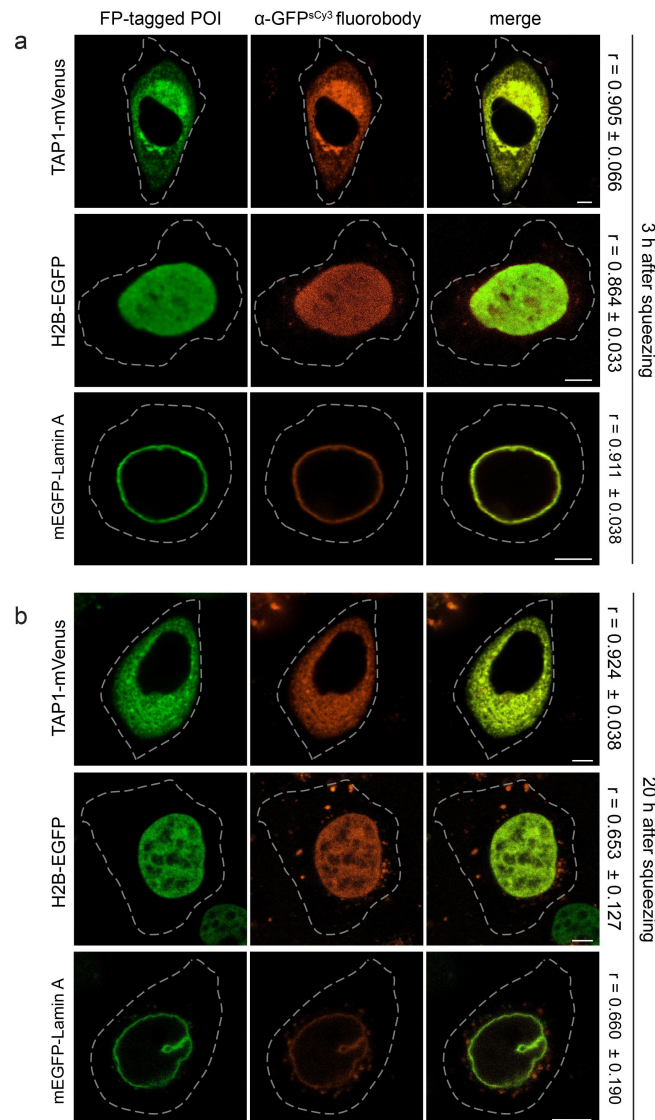
Figure 2 – Figure Supplement 2 I Live-cell labeling of FP-tagged targets via the α-GFP^{sCy3} fluorobody. α-GFP^{sCy3} Fb (200 nM) was transferred into HeLa Kyoto cells transiently transfected with TAP1-mVenus, H2B-EGFP, or mEGFP-Lamin A, respectively. Cells were imaged 3 h (**a**) and 20 h (**b**) after cell squeezing by CLSM. For all tested subcellular localizations of the FP-tagged POI, the molecular specificity of the Fb was persistent for a prolonged period of time (20 h). After 20 h, background originating as cytosolic punctae was detected. This observation is supported by a decreased Pearson´s coefficient (r, right), calculated from 8-10 individual cells. Dashed lines indicate the cell border. Scale bars: 5 µm.
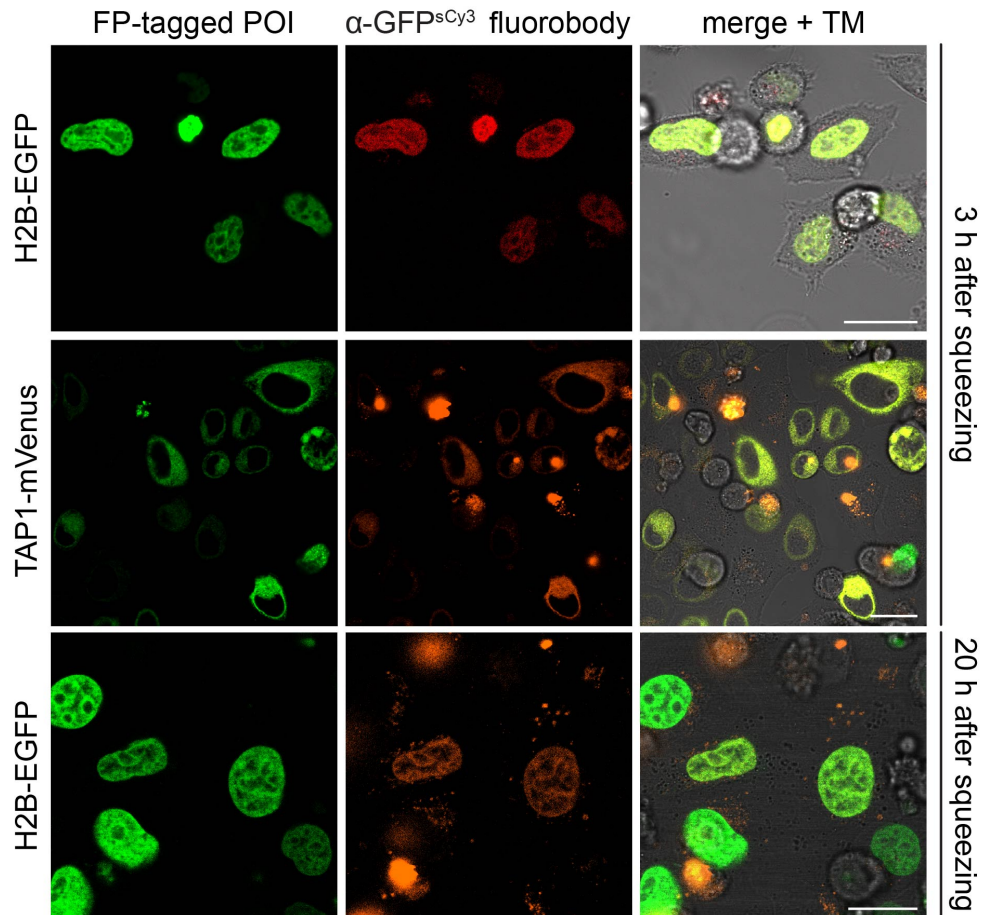
**Figure 2 – Figure Supplement 3 I High fluorescence intensity correlation between target proteins and α-GFP^{sCy3} fluorobody in living cells.** HeLa Kyoto cells expressing TAP1-mVenus or H2B-EGFP (green) were squeezed in the presence of α-GFP^{sCy3} Fb (200 nM, orange). Imaging via CLSM was performed 3 h and 20 h after squeezing. Low background and high co-localization between the Fb and POI was observed in multiple cells with varying expression level. Incipient punctual background was detectable after 20 h (bottom). Scale bars: 20 µm.

transmitted light	α-GFP^{sCy5} fluorobody	merge
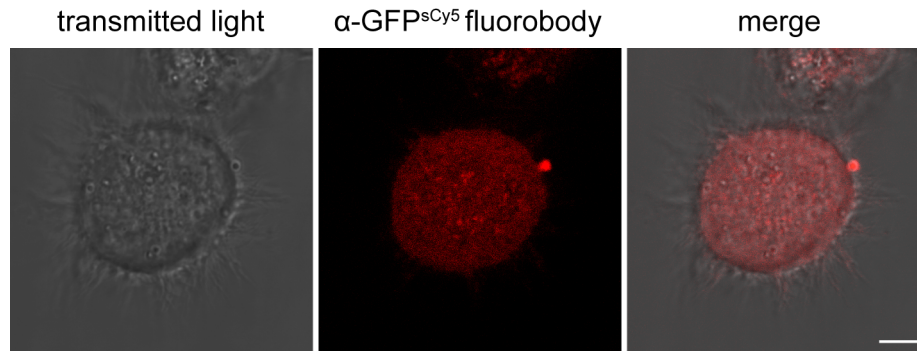
Figure 2 – Figure Supplement 4 I Cytosolic distribution of α-GFP^{sCy5} fluorobody in untransfected cells. α-GFP^{sCy5} Fb (100 nM) was delivered into HeLa Kyoto cells via cell squeezing. A cytosolic distribution of the Fb (red) was detected 1 h after squeezing. In absence of FP-tagged proteins, no distinct cellular localization of α-GFP^{sCy5} Fbs was observed, confirming the molecular specificity of the α-GFP^{sCy5} Fb for antigen tracking. Imaging was performed by CLSM. Scale bar: 5 µm.
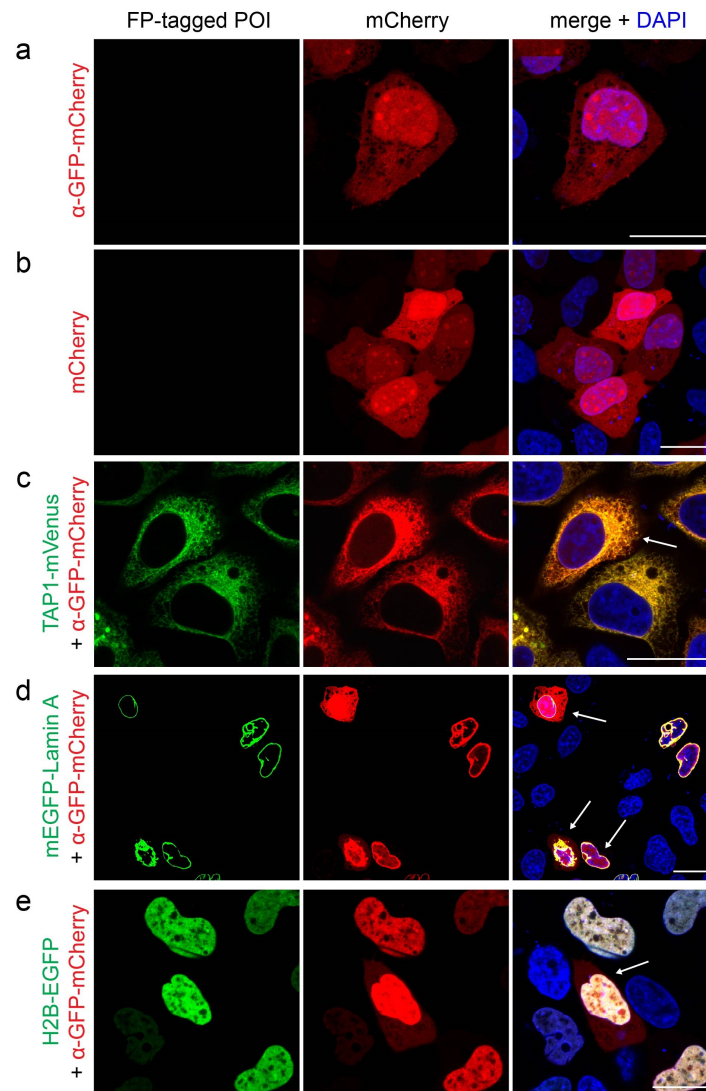
Figure 2 – Figure Supplement 5 I Transient expression of α-GFP-mCherry chromobody in mammalian cells. (**a**) In the absence of the target protein, the α-GFP-mCherry nanobody was homogenously distributed within the cytosol and nucleus, similar to mCherry alone (**b**). (**c-e**) HeLa Kyoto cells were transiently co-transfected with an α-GFP-mCherry chromobody (red) and a FP-tagged POI (TAP1-mVenus, mEGFP-Lamin A or H2B-EGFP; green). Increased chromobody expression levels resulted in a high background of unbound nanobody, distributed in the cytosol and nucleus (indicated by arrows). Before CLSM imaging, HeLa Kyoto cells were chemically arrested with 4% formaldehyde and additionally stained with DAPI (blue). Scale bars: 20 μm.

1
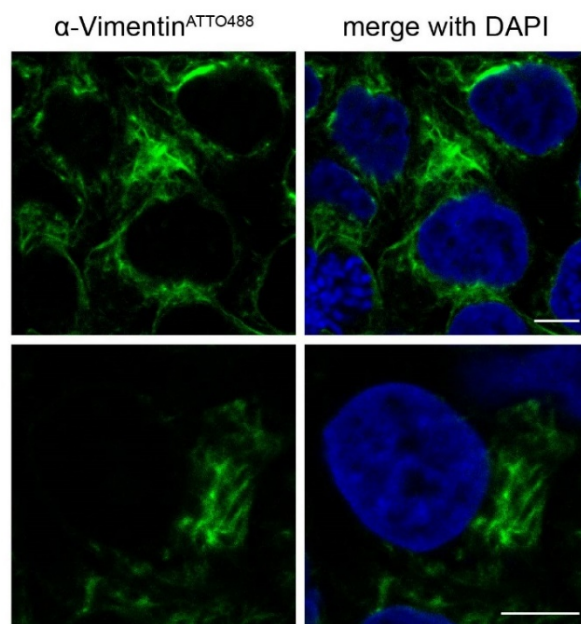
Figure 3 – Figure Supplement 1 I Vimentin staining in fixed cells. HeLa Kyoto cells were fixed,

permeabilized and stained with α-Vimentin^{ATTO488} (20 µg/ml, green) and DAPI (blue). Confocal

imaging showed specific labeling of endogenous filamentous vimentin. Scale bar: 5 µm.
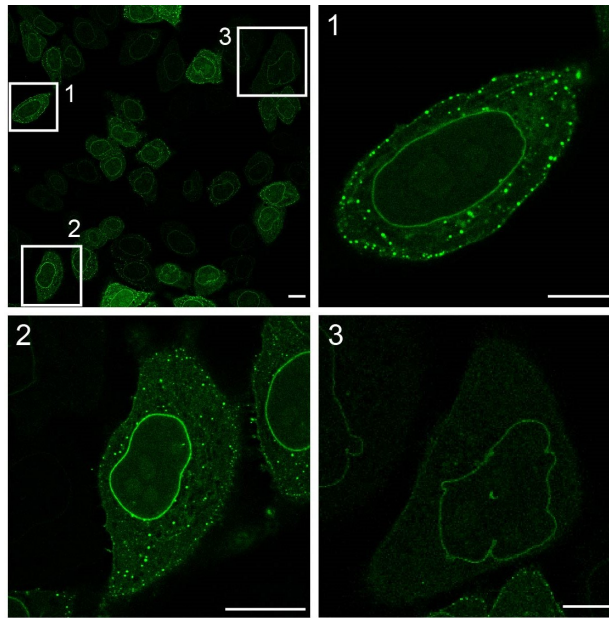
Figure 3 – Figure Supplement 2 I Transient expression of α-Lamin-EGFP chromobody in HeLa Kyoto cells entails background of free nanobody. Cells transiently transfected with α-Lamin-EGFP were fixed with 4% formaldehyde 24 h after transfection. Specific decoration of endogenous lamin at the nuclear envelope was visualized by CLSM. The variability of the chromobody expression level was accompanied by a high background, originating as cytosolic punctae. Images 1-3 are magnifications of individual cells as indicated by white boxes in the upper left image. Scale bars: 10 µm.

1
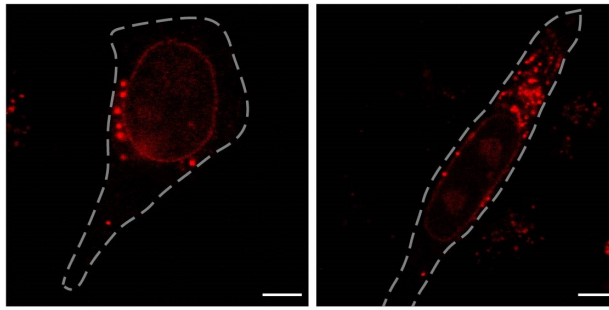
2

3 **Figure 3 – Figure Supplement 3 I Persistence of endogenous lamin targeting by Fb in living**

4 **cells.** The α-Lamin^{sCy5} Fb (500 nM) was transferred into native HeLa Kyoto cells via cell

5 squeezing. Specific decoration of the endogenous nuclear lamina by the Fb was still observed

6 20 h after squeezing by CLSM. An enriched punctual background was detected compared to 3 h

7 post squeezing (see Fig. 3a). Dashed lines indicate the cell border. Scale bars: 5 µm.
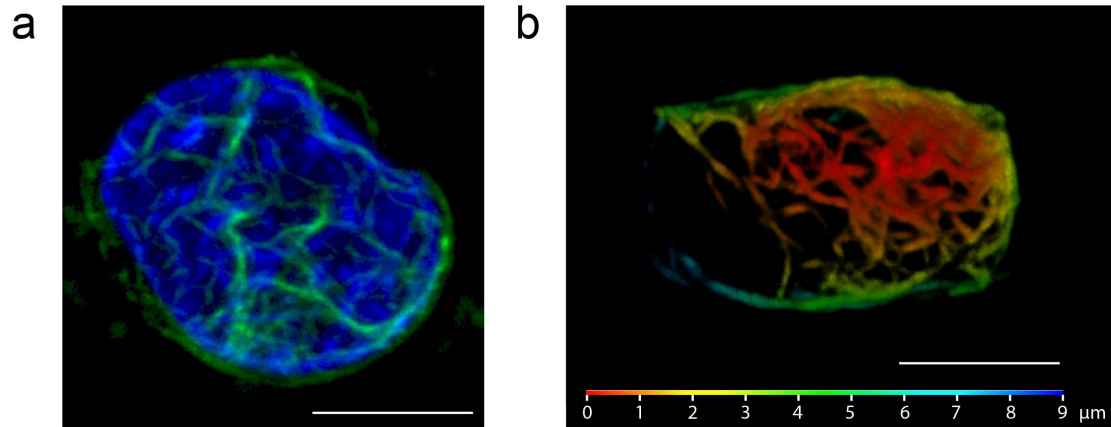
Figure 3 – Figure Supplement 4 I 3D reconstruction of endogenous vimentin network. After intracellular transfer of α-Vimentin[ATTO488] (50 µg/ml), z-stacks were recorded by confocal imaging using the Airy scan detector (SR mode, Zeiss). (**a**) Imaging was performed 3 h after squeezing with additional HOECHST staining (blue). The 3D reconstruction of the obtained z-stack showed the complex network of endogenous vimentin (green), organized around nucleus. (**b**) 3D topographic map of the endogenous vimentin meshwork. The series of z-stacks was recorded 20 h after cell squeezing and reconstructed. The rainbow-color code indicates the depth. Distance between stacks: ~ 200 nm, respectively. Scale bars: 5 µm.
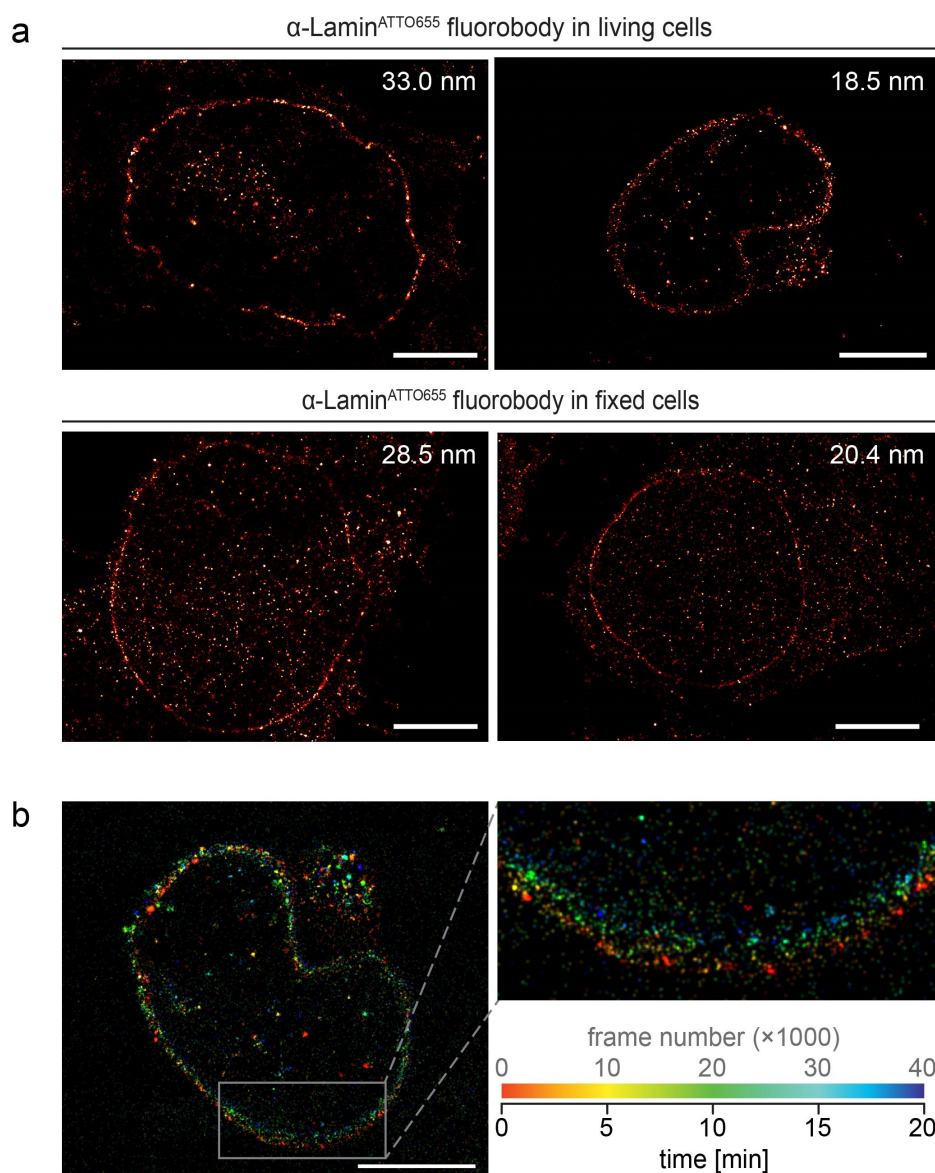
Figure 3 – Figure Supplement 5 I Super-resolution imaging of endogenous lamin in fixed and living cells. HeLa Kyoto cells were either squeezed with α-Lamin[ATTO655] Fb (500 nM) for live-cell imaging or fixed, permeabilized and stained with α-Lamin[ATTO655] Fb (100 nM). (**a**) *d*STORM analysis revealed a similar average localization precision in living (23.4 ± 8.3 nm, top) and fixed (23.2 ± 4.6 nm, bottom) cells. The localization precision determined for each image is given in the top right corner. Mean and standard deviation were calculated from three images. (**b**) Cell dynamics during live-cell super-resolution microscopy can impede imaging. Frame numbers are color-coded. Scale bar: 5 μm.

38

1   **Supplementary Video 1 I 3D reconstruction of the endogenous nuclear lamina.** After fixation

2   and permeabilization, endogenous lamin of a HeLa Kyoto cell was visualized with an

3   α-Lamin^{ATTO655} Fb (100 nM). 53 individual stacks were recorded by confocal imaging using the

4   Airy scan detector (Zeiss, distance between stacks ~ 200 nm). 3D reconstruction showed a dense

5   decoration of the complete nuclear lamina by the Fb, accompanied with a high signal-to-

6   background ratio. Several intranuclear structures of endogenous lamin were observed.